

Multiple off-axis acoustic vortices generated by dual coaxial vortex beams

Wen Li(李雯), Si-Jie Dai(戴思捷), Qing-Yu Ma(马青玉), Ge-Pu Gu(郭各朴), He-Ping Ding(丁鹤平)
Citation: Chin. Phys. B . 2018, 27(2): 024301. **doi:** 10.1088/1674-1056/27/2/024301

Journal homepage: http://cpb.iphy.ac.cn; http://iopscience.iop.org/cpb

What follows is a list of articles you may be interested in

Acoustic radiation force induced by two Airy-Gaussian beams on a cylindrical particle

Sha Gao(高莎), Yiwei Mao(毛一葳), Jiehui Liu(刘杰惠), Xiaozhou Liu(刘晓宙)
Chin. Phys. B . 2018, 27(1): 014302. **doi:** 10.1088/1674-1056/27/1/014302

Array gain for a conformal acoustic vector sensor array: An experimental study

Yong Wang(汪勇), Yi-Xin Yang(杨益新), Zheng-Yao He(何正耀), Bo Lei(雷波), Chao Sun(孙超), Yuan-Liang Ma(马远良)
Chin. Phys. B . 2016, 25(12): 124318. **doi:** 10.1088/1674-1056/25/12/124318

Multiple off-axis acoustic vortices generated by dual coaxial vortex beams*

Wen Li(李雯)[1], Si-Jie Dai(戴思捷)[2], Qing-Yu Ma(马青玉)[1,†], Ge-Pu Guo(郭各朴)[1], and He-Ping Ding(丁鹤平)[1]

[1] *Key Laboratory of Optoelectronics of Jiangsu Province, School of Physics and Technology, Nanjing Normal University, Nanjing* 210023, *China*

[2] *Honors College, Nanjing Normal University, Nanjing* 210023, *China*

(Received 29 September 2017; revised manuscript received 9 November 2017; published online 5 January 2018)

As a kind of special acoustic field, the helical wavefront of an acoustic vortex (AV) beam is demonstrated to have a pressure zero with phase singularity at the center in the transverse plane. The orbital angular momentum of AVs can be applied to the field of particle manipulation, which attracts more and more attention in acoustic researches. In this paper, by using the simplified circular array of point sources, dual coaxial AV beams are excited by the even- and odd-numbered sources with the topological charges of $l_{\rm E}$ and $l_{\rm O}$ based on the phase-coded approach, and the composite acoustic field with an on-axis center-AV and multiple off-axis sub-AVs can be generated by the superimposition of the AV beams for $|l_{\rm E}| \neq |l_{\rm O}|$. The generation of edge phase dislocation is theoretically derived and numerically analyzed for $l_{\rm E} = -l_{\rm O}$. The numbers and the topological charges as well as the locations of the center-AV and sub-AVs are demonstrated, which are proved to be determined by the topological charges of the coaxial AV beams. The proposed approach breaks through the limit of only one on-axis AV with a single topological charge along the beam axis, and also provides the feasibility of off-axis particle trapping with multiple AVs in object manipulation.

Keywords: dual coaxial acoustic vortex (AV) beams, multiple off-axis AVs, on-axis center-AV, topological charge, phase-coded approach

PACS: 43.25.Qp, 43.60.Fg, 43.38.Hz **DOI:** 10.1088/1674-1056/27/2/024301

1. Introduction

As is well known, the acoustic vortex (AV)[1–5] is a special sound beam with cross-sectional distributions of circular pressure and helical phase. Along the central axis, the acoustic pressure of the wave front is zero, exhibiting a typical hollow structure. A phase factor $\exp(\mathrm{i}l\theta)$ is often used to describe the speed of phase rotation around the azimuth angle θ, where l is the topological charge,[6] denoting the phase change of $2\pi l$ around the vortex core with the polarity[7] indicating the clockwise or anti-clockwise phase spiral of the helical wavefront. Due to the capability of the orbital angular momentum (OAM)[8] transfer to matter, the topological structure of AVs exhibits great significance in the applications of particle trapping and object rotation.[9–14] In the past few decades, several designs, such as the acoustic spanner and acoustic tweezers,[15–19] have been developed to realize particle manipulation by utilizing the AV propagating along the center axis. To enlarge the trapping area with improved accuracy, new investigations on the generation of composite AV fields have been carried out. In optics, by employing the techniques of helical phase spatial filtering,[20] superposition of two coherent beams,[21] motion control of multi-vortex beams,[22] coaxial superimposition of two Laguerre–Gauss beams[23–25] based on the Gouy phase, several methods have been used to form composite optical vortex (OV) fields and realize synchronized multi-region particle manipulation in the transverse plane. Compared with an OV beam, besides the continuous phase spiral, an AV beam[26,27] has a long wavelength with a deep penetration depth[28] and a little biological loss[29] in biomedical tissues. A higher acoustic radiation force of AVs with stronger moments[30] can improve the ability[31] to manipulate an object for non-magnetic or non-conducting material,[32] resulting in particle capture and transport inside the body.

In order to form a multi-region composite AV field to break through the limit of there being only one on-axis AV with a single topological charge[33] along the beam axis, a superimposition algorithm for multiple off-axis AVs using dual coaxial AV beams is proposed in this paper. Based on the configuration of a circular array of sparse point sources, two coaxial AV beams along the same propagation direction at an identical frequency are produced first by the even- and odd-numbered sources through using the phase-coded approach.[34–37] With the superimposition effect of the two AV beams, a composite acoustic field with an on-axis center-AV and multiple off-axis sub-AVs is generated, realizing the

*Project supported by the National Natural Science Foundation of China (Grant Nos. 11474166 and 11604156), the Science and Technology Cooperation Projects of People's Republic of China–Romania (Grant No. 42-23), the Natural Science Foundation of Jiangsu Province, China (Grant No. BK20161013), the Postdoctoral Science Foundation of China (Grant No. 2016M591874), and the Priority Academic Program Development of Jiangsu Higher Education Institutions, China.

†Corresponding author. E-mail: maqingyu@njnu.edu.cn

© 2018 Chinese Physical Society and IOP Publishing Ltd

topological energy transfer from the center to the surrounding area. The generation of edge phase dislocation[38,39] is also theoretically derived and numerically analyzed. With theoretical simulations, the generation rule of multiple off-axis AVs is summarized, and the numbers and the topological charges as well as the positions of the center-AV and sub-AVs are demonstrated to be determined by the topological charges of the coaxial AV beams. The favorable results provide the theoretical basis for the formation of multiple off-axis AVs, and suggest the potential applications in object manipulation, especially for the radiation force based particle trapping and three-dimensional (3D) object driving using AVs in biomedical engineering.

2. Principle and method

The schematic diagram of the generation system of multiple off-axis AVs using dual coaxial AV beams is illustrated in Fig. 1. The $2N$ acoustic sources are distributed uniformly on a circumference with a radius a. Supposing the radius of the sources is far less than the wave length, each source can be considered as a point source to produce a typical spherical radiation in free space. The $2N$ sources can be divided into the even- and odd-numbered groups. By applying the phase-coded approach to the N even-numbered sources, an AV beam with an obvious pressure zero along the center axis can be generated and the topological charge l_{E} is determined by the initial phase difference between adjacent sources. With a similar excitation sequence for the N odd-numbered sources at an identical frequency, a similar AV beam propagating along the beam axis with the topological charge l_{O} can also be produced. And then, a composite acoustic field with multiple off-axis AVs can be formed by the superimposition of the two coaxial AV beams.

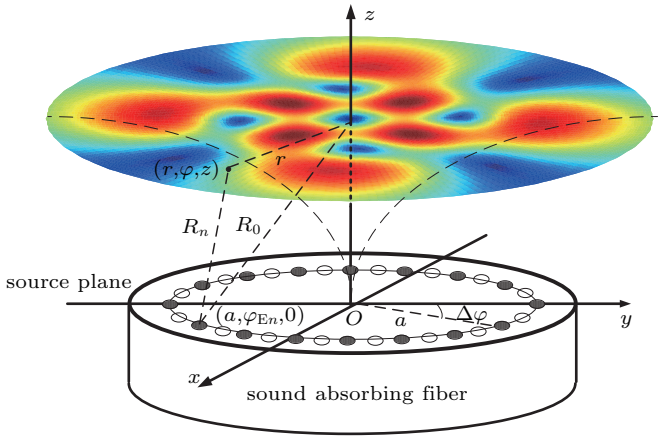


Fig. 1. (color online) Schematic diagram of the generation system of multiple off-axis AVs by using dual coaxial AV beams.

As is well known, under the excitation of an electrical signal at the frequency f, the acoustic pressure produced by a point source at $(a,\varphi,0)$ can be calculated by $p(a,\varphi,0,t) = A\exp(-\mathrm{i}\omega t)\exp(\pm\mathrm{i}\phi)$, where A is the pressure amplitude, $\omega = 2\pi f$ is the angular frequency, and ϕ is the initial phase of the acoustic wave. Therefore, the acoustic pressure at (r,φ,z) generated by the source can be described by

$$p(r,\varphi,z,t) = \frac{A}{R}\exp(-\mathrm{i}\omega t)\exp(\mathrm{i}kR)\exp(\pm\mathrm{i}\phi), \tag{1}$$

where $k = \omega/c$ is the wave number for the sound speed c, and R is the transmission distance between $(a,\varphi,0)$ and (r,φ,z).

In order to generate an AV beam with a controllable topological charge, the accurate coordinates and the corresponding initial phases of the sources should be taken into account. For the $2N$ sources in the system, the spatial angle difference between adjacent sources is $\Delta\varphi = \pi/N$. By setting the pressure amplitude and the phase difference of the N even-numbered sources to be A_{E} and $\Delta\phi_{\mathrm{E}} = l_{\mathrm{E}}2\Delta\varphi$, the spatial angle and the initial phase of the nth even-numbered source are $\varphi_{\mathrm{E}n} = 2\pi(n-1)/N$ and $\phi_{\mathrm{E}n} = 2l_{\mathrm{E}}\pi(n-1)/N$, and the total phase shift of the N sources is $2\pi l_{\mathrm{E}}$. Then, the pressure at (r,φ,z) generated by the N even-numbered sources can be calculated from

$$p_{\mathrm{E}}(r,\varphi,z,t) = \exp(-\mathrm{i}\omega t)\sum_{n=1}^{N}\frac{A_{\mathrm{E}}}{R_n}\exp(\mathrm{i}kR_n)\exp(\pm\mathrm{i}\phi_{\mathrm{E}n}). \tag{2}$$

For an even-numbered source, the transmission distance can be calculated from

$$R_n = \sqrt{\{r\cos\varphi - a\cos\varphi_{\mathrm{E}n}\}^2 + \{r\sin\varphi - a\sin\varphi_{\mathrm{E}n}\}^2 + z^2},$$

which can be rewritten as

$$R_n \approx \sqrt{a^2+z^2} + \frac{r^2 - 2ra\cos(\varphi-\varphi_{\mathrm{E}n})}{2\sqrt{a^2+z^2}}$$

for paraxial simplification, where $R_0 = \sqrt{a^2+z^2}$ is the distance between the n-th even-numbered source and $(0,0,z)$. By taking the approximation of $R_n \approx R_0$ only for acoustic pressure, equation (2) can be rewritten as

$$\begin{aligned} p_{\mathrm{E}}(r,\varphi,z,t) = {} & \frac{A_{\mathrm{E}}}{R_0}\exp(-\mathrm{i}\omega t)\sum_{n=1}^{N}\exp \\ & \times\left[\mathrm{i}kR_0 + \frac{\mathrm{i}kr^2}{2R_0} - \frac{\mathrm{i}kra}{R_0}\cos(\varphi-\varphi_{\mathrm{E}n})\right] \\ & \times\exp(\pm\mathrm{i}\phi_{\mathrm{E}n}). \end{aligned} \tag{3}$$

After further formula transformation, the acoustic pressure of the AV beam generated by the even-numbered sources can be simplified into

$$\begin{aligned} p_{\mathrm{E}}(r,\varphi,z,t) = {} & \frac{A_{\mathrm{E}}}{R_0}\exp\left[\mathrm{i}\left(kR_0 + \frac{kr^2}{2R_0} - \omega t\right)\right] \\ & \times\sum_{n=1}^{N}\exp\left[\frac{-\mathrm{i}kra}{R_0}\cos(\varphi-\varphi_{\mathrm{E}n})\right] \\ & \times\exp(\pm\mathrm{i}\varphi_{\mathrm{E}n}). \end{aligned} \tag{4}$$

As reported in our previous studies,[34–37] by applying the phase-coded approach to the circular source array, the AV

beam can be generated along the center axis with a controllable topological charge. In a transverse plane, there is an obvious pressure null at the center to form the vortex core of the AV. With the increase of the radial distance, the acoustic pressure increases accordingly until it reaches the first peak, and then goes down gradually. Around the vortex core, circular pressure distributions with perfect phase spirals can be produced. The maximal topological charge of the AV beam generated by the N even-numbered sources is proved to be fix$[(N-1)/2]$, where fix(x) rounds the element x toward zero.

Similarly, by repeating the phase-coded approach for the N odd-numbered sources, the coaxial AV beam with the topological charge l_{O} at the same frequency $f$can also be generated. For the odd-numbered sources, the pressure amplitude and the initial phase are set to be A_{O} and $\phi_{\mathrm{O}n}$, respectively, and the phase difference between adjacent odd-numbered sources set to be $\Delta\phi_{\mathrm{O}} = 2l_{\mathrm{O}}\Delta\varphi$ with a total phase shift of $2\pi l_{\mathrm{O}}$. By considering the spatial angle difference π/N between the adjacent sources, the spatial angle and the initial phase of the n-th odd-numbered source are obtained to be $\varphi_{\mathrm{O}n} = \varphi_{\mathrm{E}n} + \pi/N$ and $\phi_{\mathrm{O}n} = 2l_{\mathrm{O}}\pi(n-1)/N$. Hence, by considering the initial phase difference $\Delta\phi$, the acoustic pressure of the AV beam generated by the odd-numbered sources can be expressed as

$$\begin{aligned} p_{\mathrm{O}}(r,\varphi,z,t) = {} & \frac{A_{\mathrm{O}}}{R_0}\exp\left[\mathrm{i}\left(kR_0+\frac{kr^2}{2R_0}-\omega t\right)\right] \\ & \times\sum_{n=1}^{N}\exp\left[\frac{-\mathrm{i}kra}{R_0}\cos(\varphi-\varphi_{\mathrm{O}n})\right] \\ & \times\exp(\pm\mathrm{i}\phi_{\mathrm{O}n}+\mathrm{i}\Delta\phi). \end{aligned} \tag{5}$$

Then, by applying the phase-coded approach to the even- and odd-numbered sources simultaneously, the pressure of the composite acoustic field can be calculated by the superimposition of the coaxial AV beams as

$$p(r,\varphi,z,t) = p_{\mathrm{E}}(r,\varphi,z,t) + p_{\mathrm{O}}(r,\varphi,z,t). \tag{6}$$

Therefore, the distribution of the multiple off-axis AVs can be calculated based on Eq. (6) for the coaxial AV beams with various topological charges. The cross-sectional pressure distribution of the composite acoustic field generated by the two coaxial AV beams with $l_{\mathrm{E}} = 1$ and $l_{\mathrm{O}} = -3$ presented in Fig. 1 shows a center-AV at the center axis and 4 sub-AVs around, demonstrating the feasibility of generating an on-axis center-AV and multiple off-axis AVs using the dual coaxial AV beams.

3. Numerical studies

To analyze the characteristics of the multiple off-axis AVs generated by dual coaxial AV beams quantitatively, numerical studies were performed in free space at $f = 1.15$ kHz. The circumference radius of the source array was set to be $a = 30$ cm, which corresponds to the wave length for $c = 344$ m/s in air, and the observation height was set to be $z = 20$ cm to study the transverse distributions of pressure and phase. The source number was set to be $2N = 32$ and the pressure amplitudes were set to be $A_{\mathrm{E}} = A_{\mathrm{O}}$ to simplify the parameter control of the system. As is well known, when topological charges of the two AV beams generated by the even- and odd-numbered sources are the same as $l_{\mathrm{E}} = l_{\mathrm{O}}$, no off-axis AVs can be formed by the fixed phase difference. Meanwhile, obvious phase dislocations can also be produced by the AVs with $l_{\mathrm{E}} = -l_{\mathrm{O}}$. Therefore, the even- and odd-numbered sources placed around the circumference are used to generate the coaxial AV beams with different topological charges for $|l_{\mathrm{E}}| \neq |l_{\mathrm{O}}|$.

The cross-sectional distributions of pressure and phase of the AV beam with $l_{\mathrm{E}} = 1$ generated by the even-numbered sources were simulated as plotted in Figs. 2(a) and 2(b). Circular pressure distributions are clearly displayed in Fig. 2(a) with a clear pressure null at the origin to form the vortex core. With the increase of the radius r, the acoustic pressure increases accordingly to its maximum at $r \approx 10$ cm. Meanwhile, due to the superimposition effect of the 16 phase-coded acoustic waves, an obvious phase singularity is visualized at the origin in Fig. 2(b), and an anti-clockwise phase spiral from 0 to 2π in one circle around the vortex core is clearly displayed, demonstrating the existence of the AV with $l_{\mathrm{E}} = 1$. Then, by changing the initial phase difference for the odd-numbered sources, the corresponding distributions of the AV beam with $l_{\mathrm{O}} = -3$ were also simulated as shown in Figs. 2(c) and 2(d). For the higher topological charge, an enlarged AV is clearly shown in the center region with a bigger radius of circular pressure peak in Fig. 2(c). Around the vortex core, a clockwise phase spiral is also observed in Fig. 2(d) with three times phase variation from 0 to 2π, proving the formation of the AV beam with $l_{\mathrm{O}} = -3$. Thus, the topological polarity of the AVs in the transverse plane can be identified by the direction of the phase spiral from 0 to 2π around the vortex core, where the positive and negative polarities are defined as the anti-clockwise and clockwise direction of phase spirals, respectively.

Based on Eq. (6), the cross-sectional distributions of pressure and phase of the composite acoustic field were simulated as plotted in Figs. 2(e) and 2(f). Besides the center-AV with $l_{\mathrm{c}} = 1$ (anti-clockwise phase spiral) centered at the origin, four sub-AVs with $l_{\mathrm{s}} = -1$ (clockwise phase spiral) are located uniformly around the origin with the radius R_{V} (distance from the origin to the center of a sub-AV) of 18.25 cm. Around the vortex core of each sub-AV, a phase spiral with a clockwise phase variation from 0 to 2π is clearly displayed, which is opposite to the spiral direction of the center-AV. It is worth noting that the obvious distributions of non-circular pressure and bended radial phase[23–25] can be observed in sub-AVs, which are produced by the different radial pressure distributions of the coaxial AV beams with different topological charges.

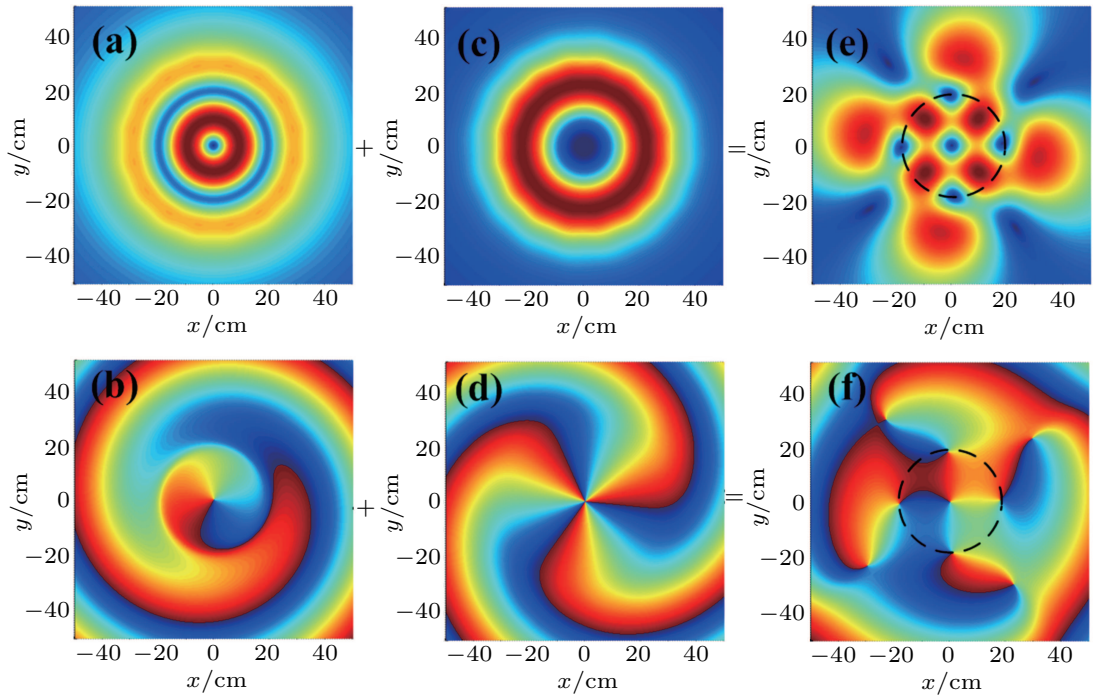


Fig. 2. (color online) Cross-sectional distributions of pressure and phase at $z = 20$ cm generated by the coaxial AV beams with ((a) and (b)) $l_{\mathrm{E}} = 1$, ((c) and (d)) $l_{\mathrm{O}} = -3$, and ((e) and (f)) superimposed multiple off-axis AVs.

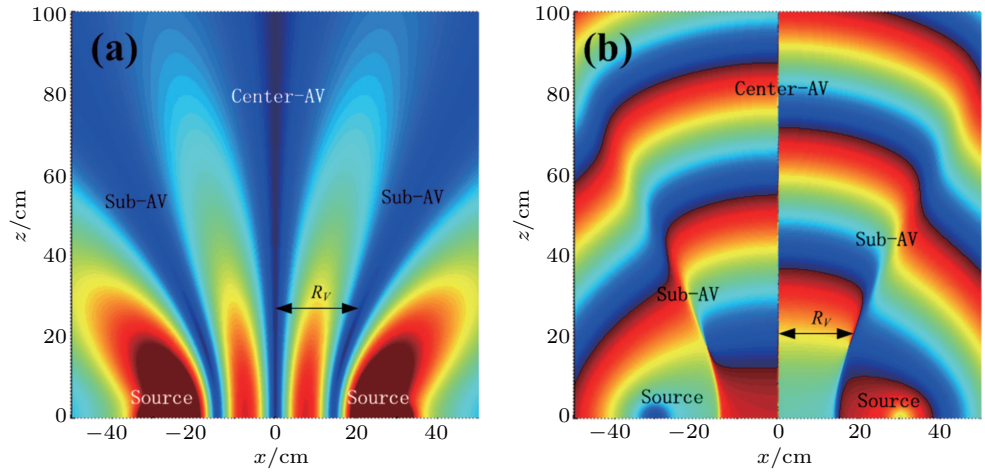


Fig. 3. (color online) Axial profiles of (a) pressure and (b) phase of the acoustic field with multiple off-axis AVs.

In order to summarize the generation rule of multiple off-axis AVs, the axial profiles of pressure and phase of the composite acoustic field were simulated as plotted in Figs. 3(a) and 3(b), which exhibit good symmetry around the center axis. In the source plane ($z = 0$), two divergent acoustic beams radiated from the two sources are clearly displayed with an identical pressure and opposite phases, and the acoustic pressure decreases with the increase of the transmission distance. Besides the gradually increased radius of the central-AV along the center axis, two sub-AVs with expanded vortex radius are also displayed with a gradually increased R_{V}. Corresponding to Figs. 3(a) and 3(b), the acoustic pressure along the center axis is 0 with an obvious phase shift π to form the center-AV. Meanwhile, along the trajectory of vortex cores of sub-AVs, significant tangential phase shifts can also be identified, demonstrating an expanded R_{V} of off-axis sub-AVs.

In addition, further studies on the characteristics of the multiple off-axis AVs generated by two coaxial AV beams with different topological charges were conducted. For the cross-sectional distributions of pressure and phase generated by the coaxial AV beams with $l_{\mathrm{E}} = -1$ and $l_{\mathrm{O}} = -3$ as shown in Figs. 4(a) and 4(b), beside the center-AV with $l_{\mathrm{c}} = -1$ located at the origin, two sub-AVs with $l_{\mathrm{s}} = -1$ are also displayed with $R_{\mathrm{V}} = 18$ cm (indicated by the dashed circle). By changing the topological charges of the coaxial AV beams to $l_{\mathrm{E}} = 2$ and $l_{\mathrm{O}} = -4$, the cross-sectional distributions of the composite acoustic field are illustrated in Figs. 4(c) and 4(d). An expanded center-AV with $l_{\mathrm{c}} = 2$ can be observed in the center region with 6 detached sub-AVs located around with $l_{\mathrm{s}} = -1$ and $R_{\mathrm{V}} = 27$ cm.

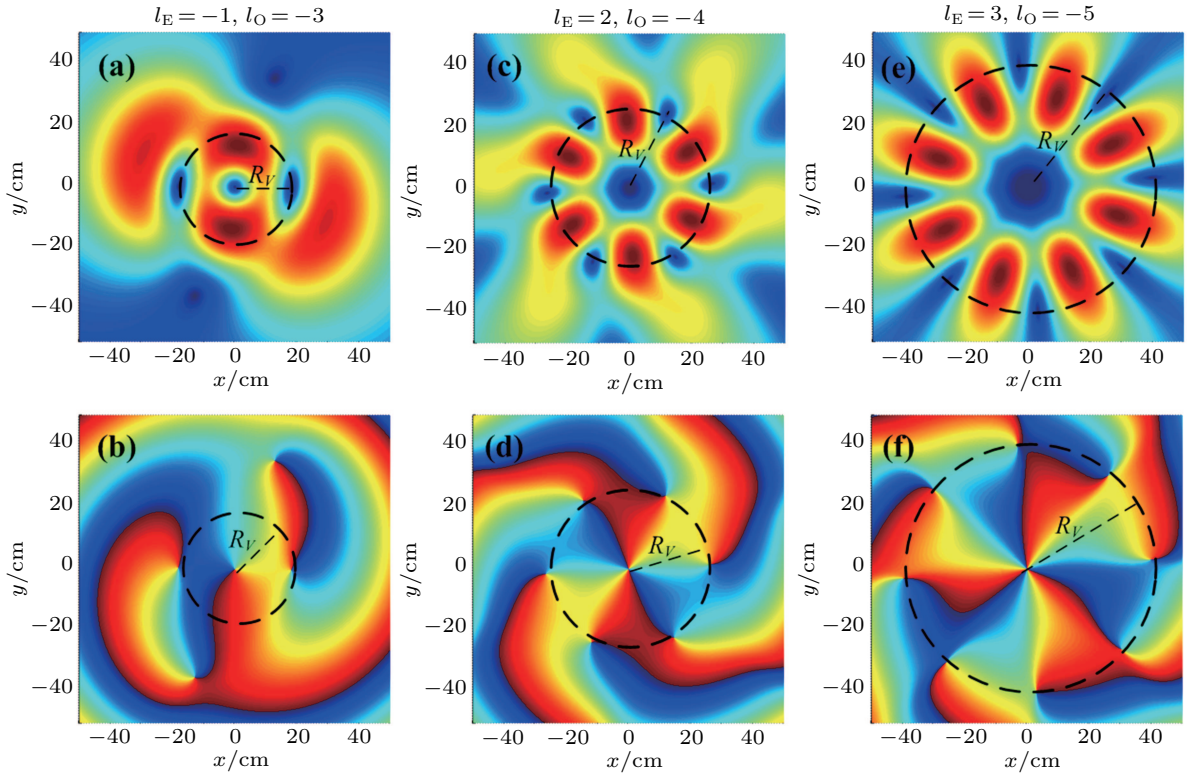


Fig. 4. (color online) Cross-sectional distributions of pressure and phase of off-axis AVs at $z = 20$ cm for the coaxial AV beams with ((a) and (b)) $l_E = -1$ and $l_O = -3$, ((c) and (d)) $l_E = 2$ and $l_O = -4$, and ((e) and (f)) $l_E = 3$ and $l_O = -5$.

Based on the simulation results of the coaxial AV beams with different topological charges for $|l_E| \neq |l_O|$ as presented above, it can be concluded that a center-AV can be generated along the center axis with the topological charge of $\min(|l_E|, |l_O|)$ and the topological polarity of $\text{sign}(l_E + l_O)$. The number of the superimposed multiple off-axis sub-AVs is proved to be $|l_E - l_O|$ and the topological charge of sub-AVs is 1 with the topological polarity of $\text{sign}(1/l_E + 1/l_O)$. Corresponding to the origin in the transverse plane, the azimuth angle between the vortex cores of adjacent sub-AVs is $2\pi/|l_E - l_O|$. The detailed relationship between the topological charges of the coaxial AV beams and the characteristics of the multiple off-axis AVs is listed in Table 1. Therefore, with the known parameters l_E and l_O of the coaxial AV beams, the number of sub-AVs, the topological charges l_c and l_s of the center-AV and sub-AVs can be predicted accurately. The formation rule of multiple off-axis AVs is further verified by the superimposition results generated by the AV beams with bigger topological charges of $l_E = 3$ and $l_O = -5$ as shown in Figs. 4(e) and 4(f). Eight ($|l_E - l_O|$) sub-AVs are clearly displayed around the origin, and the topological charges of the center-AV and sub-AVs are $l_c = 3$, which is the same as the topological charge of l_E, and $l_s = -1$, which is the same as the topological polarity of l_O, respectively. However, since R_V (about 40 cm) of sub-AVs is bigger than a (30 cm), the pressure distribution of each sub-AV exhibits an unclosed emanating state along the corresponding radial direction.

Table 1. Relationship between the topological charges of the dual coaxial AV beams and the properties of the multiple off-axis AVs of the composite acoustic field.

AV type \ Properties	Number of AV	Topological charge	Topological polarity
sub-AV	$\|l_E - l_O\|$	1	$\text{sign}(l_E + l_O)$
center-AV	1	$\min(\|l_E\|, \|l_O\|)$	$\text{sign}(1/l_E + 1/l_O)$

With the simulation results as presented above, one can obtain that the composite acoustic field of multiple off-axis AVs is the superimposition of dual coaxial AV beams with the topological charges of l_E and l_O. To analyze R_V of sub-AVs, the radial pressure distributions for the even- or odd-numbered AV beam with $l = 1$ to 7 are calculated as plotted in Fig. 5. It is obvious that a bigger radius of the first pressure peak of the AV with lower acoustic pressure can be generated for high l: the radius increases from 10.75 cm to 48.0 cm with l increasing from 1 to 7. Therefore, in the paraxial region, the AV beams can be generated by the even- and odd-numbered sources, and the transverse pressure dis-

tributions of AVs can be described by $p_{\mathrm{E}}(l_{\mathrm{E}},r)\exp(\mathrm{i}l_{\mathrm{E}}\varphi)$ and $p_{\mathrm{O}}(l_{\mathrm{O}},r)\exp(\mathrm{i}l_{\mathrm{O}}\varphi+\mathrm{i}\Delta\varphi)$, where $p_{\mathrm{E}}(l_{\mathrm{E}},r)$ and $p_{\mathrm{O}}(l_{\mathrm{O}},r)$ can be obtained from Fig. 5(a). By adjusting the angle difference $\Delta\varphi$ between the AV beams generated by the even- and odd-numbered sources, there must be positions with $|p(r,\varphi)| = |p_{\mathrm{E}}(l_{\mathrm{E}},r)\exp(\mathrm{i}l_{\mathrm{E}}\varphi)+p_{\mathrm{O}}(l_{\mathrm{O}},r)\exp(\mathrm{i}l_{\mathrm{O}}\varphi+\mathrm{i}\Delta\varphi)| = 0$, indicating the formation of the vortex cores of sub-AVs. To make $|p(r,\varphi)|=0$, the acoustic pressures of $p_{\mathrm{E}}(l_{\mathrm{E}},r)$ and $p_{\mathrm{O}}(l_{\mathrm{O}},r)$ should be at the same amplitude with a phase difference of π, which might be realized by the intersection of two curves in Fig. 5(a). Hence, for the coaxial AVs with higher topological charges, a bigger R_{V} from the beam center to the vortex core of the sub-AV can be produced. For example, the radial pressure distributions generated by the coaxial AV beams with $l_{\mathrm{E}}=1$ and $l_{\mathrm{O}}=5$ at different values of $\Delta\varphi$ are illustrated in Fig. 5(b). For different values of $\Delta\varphi$, a similar center-AV ($l_{\mathrm{c}}=1$) is shown in the center region with a similar radius ($r<11$ cm) of the first pressure peak. By adjusting $\Delta\varphi$ from 0 to $\pi/2$, a minimum pressure of almost zero is visualized at $R_{\mathrm{V}}=22.8$ cm when $\Delta\varphi=\pi/4$, indicating the accurate location of the vortex core of sub-AVs. By increasing the topological charges to $l_{\mathrm{E}}=2$ and $l_{\mathrm{O}}=5$, the variations of radial pressure with $\Delta\varphi$ are illustrated in Fig. 5(c). A bigger center-AV located at the origin with $l_{\mathrm{c}}=2$ is displayed with the pressure peak at $r=16.8$ cm, and several sub-AVs can be generated at $R_{\mathrm{V}}=30.2$ cm when $\Delta\varphi=\pi$. In addition, with the simulation results for the dual coaxial AV beams with different topological charges, it can also be observed that the accurate locations of the vortex cores of sub-AVs are determined by the comprehensive parameters of the system, including the array radius, working frequency, topological charges, spatial angle difference, initial phase difference, etc. In a word, the radius of R_{V} is proved to be located between the maximum radius and minimum radius of the pressure peaks of each of the two coaxial AV beams, i.e., $\min(R_{l_{\mathrm{E}}},R_{l_{\mathrm{O}}})<R_{\mathrm{V}}<\max(R_{l_{\mathrm{E}}},R_{l_{\mathrm{O}}})$. In practical applications, the radius R_{V} of sub-AVs is more meaningful and valuable than the azimuth angle, because the azimuth angle can be positioned precisely by adjusting the initial phase difference between the even- and odd-numbered sources.

In addition, a special case for the coaxial AV beams with $l_{\mathrm{E}}=-l_{\mathrm{O}}$ is noticeable. The pressure of the composite acoustic field in the observation plane can be expressed as $p(r,\varphi)=p_{\mathrm{E}}(l_{\mathrm{E}},r)\exp(\mathrm{i}l_{\mathrm{E}}\varphi)+p_{\mathrm{E}}(l_{\mathrm{E}},r)\exp(-\mathrm{i}l_{\mathrm{E}}\varphi+\mathrm{i}\Delta\varphi)$, and it can be simplified into

$$p(r,\varphi)=p_{\mathrm{E}}(l_{\mathrm{E}},r)[\exp(\mathrm{i}l_{\mathrm{E}}\varphi)+\exp(-\mathrm{i}l_{\mathrm{E}}\varphi+\mathrm{i}\Delta\varphi)]. \quad (7)$$

By defining $|\exp(\mathrm{i}l_{\mathrm{E}}\varphi)+\exp(-\mathrm{i}l_{\mathrm{E}}\varphi+\mathrm{i}\Delta\varphi)|=0$ for an arbitrary pressure $p_{\mathrm{E}}(l_{\mathrm{E}},r)$, the specific angles at $(2m+1)\pi/(2l_{\mathrm{E}})+\Delta\varphi/(2l_{\mathrm{E}})$ for $m=0,1,2,3,\ldots,2|l_{\mathrm{E}}|-1$ around the origin can be achieved to form pressure-zero lines of edge phase dislocation along the radial direction. Therefore, for the AV beams with topological charges of l_{E} and $-l_{\mathrm{E}}$, $2|l_{\mathrm{E}}|$ lines with zero pressure and edge phase dislocation can be produced from the origin. Based on Eq. (7), circular pressure distributions generated by the two coaxial AV beams of $l_{\mathrm{E}}=3$ and $l_{\mathrm{O}}=-3$ with the initial spatial angles of 0°, −30°, and −60° are plotted in Fig. 6(a). For $\Delta\varphi=0$, six pressure-zero lines at $\varphi=30°$, 90°, and 150° are clearly displayed. By increasing $\Delta\varphi$, obvious angle shift of $\Delta\varphi/6$ can also be identified. In addition, for the simulations with $l_{\mathrm{E}}=5$ and $l_{\mathrm{O}}=-5$ as shown in Fig. 6(b), the generation rule of edge phase dislocation is further demonstrated by ten pressure-zero lines of edge phase dislocation with the corresponding angle shift of $\Delta\varphi/10$. Whereas for the helical spirals of the coaxial AV beams along the propagation axis, the specific angles of edge phase dislocations are different at different transmission distances with an angle shift of $\pi/(|l_{\mathrm{E}}|)$ between the adjacent edge phase dislocations.

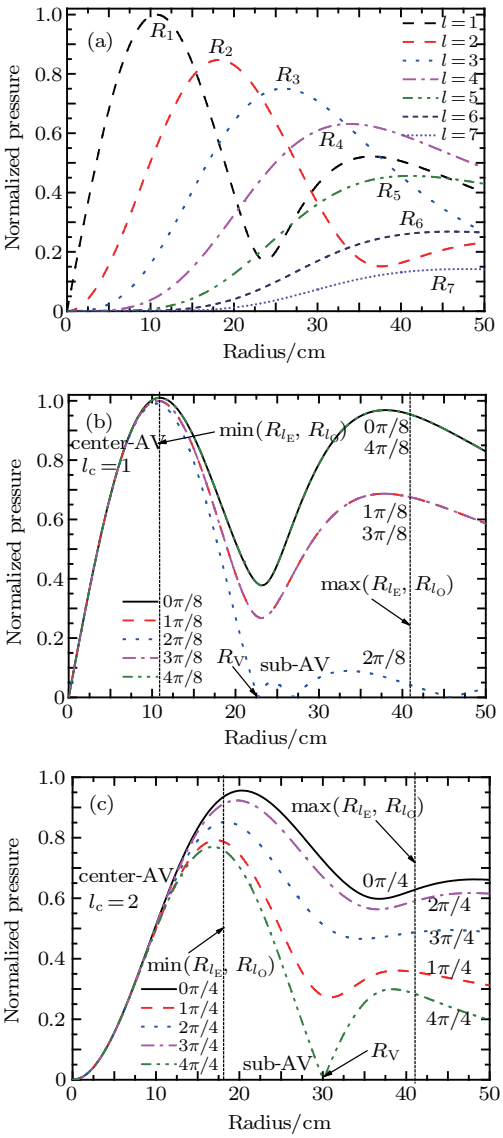


Fig. 5. (color online) (a) Radial pressure distributions at $z=20$ cm generated by the even- and odd-numbered AV with $l=1$ to 7, and the corresponding radial pressure distributions generated by the coaxial AV beams with (b) $l_{\mathrm{E}}=1$ and $l_{\mathrm{O}}=5$, and (c) $l_{\mathrm{E}}=2$ and $l_{\mathrm{O}}=5$ for different values of $\Delta\varphi$.

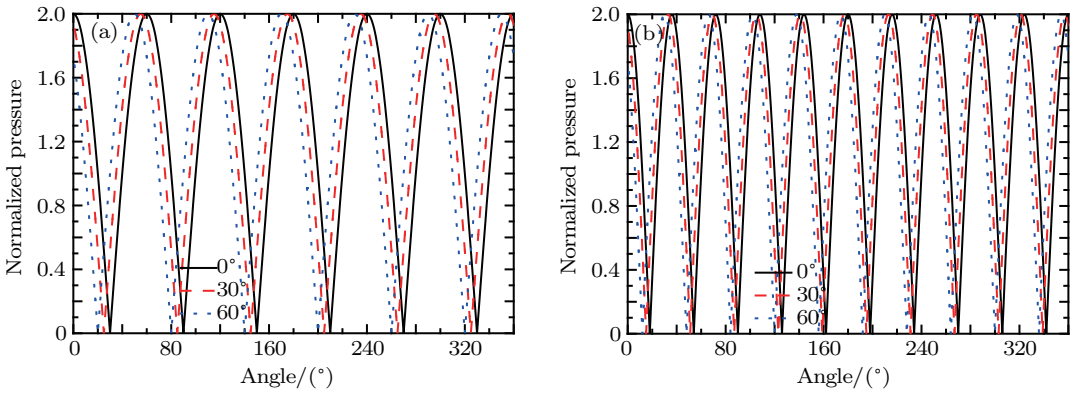


Fig. 6. (color online) Circular pressure distributions at $z = 20$ cm generated by the coaxial AV beams with (a) $l_{\mathrm{E}} = 3$ and $l_{\mathrm{O}} = -3$, and (b) $l_{\mathrm{E}} = 5$ and $l_{\mathrm{O}} = -5$ for the initial spatial angles of 0°, −30°, and −60°.

By setting $l_{\mathrm{E}} = 3$ and $l_{\mathrm{O}} = -3$ to the coaxial AV beam with $\Delta\varphi = \pi/16$, the cross-sectional distributions of pressure and phase are simulated as illustrated in Figs. 7(a) and 7(b). Six sectors are clearly displayed in Fig. 7(a), which are divided by six pressure-zero lines along the radial direction from the origin. A pressure peak can also be identified in each sector without the generation of an AV inside. Corresponding to Fig. 7(a), six phase sectors divided by six edge phase dislocations with a phase shift of π can also be observed in Fig. 7(b). Then, the generation of edge phase dislocations is also proved by the ten-sector distributions in Figs. 7(c) and 7(d) for the coaxial AV beams with $l_{\mathrm{E}} = 5$ and $l_{\mathrm{O}} = -5$. In addition, by adjusting the initial angle difference $\Delta\varphi$ between the even- and odd-numbered sources, except for a certain angle of image rotation around the origin, similar distributions of pressure and phase with obvious edge phase dislocations are achieved, demonstrating that $2\,|l_{\mathrm{E}}|$ edge phase dislocations with pressure zero can be generated by the AV beams for $l_{\mathrm{E}} = -l_{\mathrm{O}}$ with less influence of the initial angle difference.

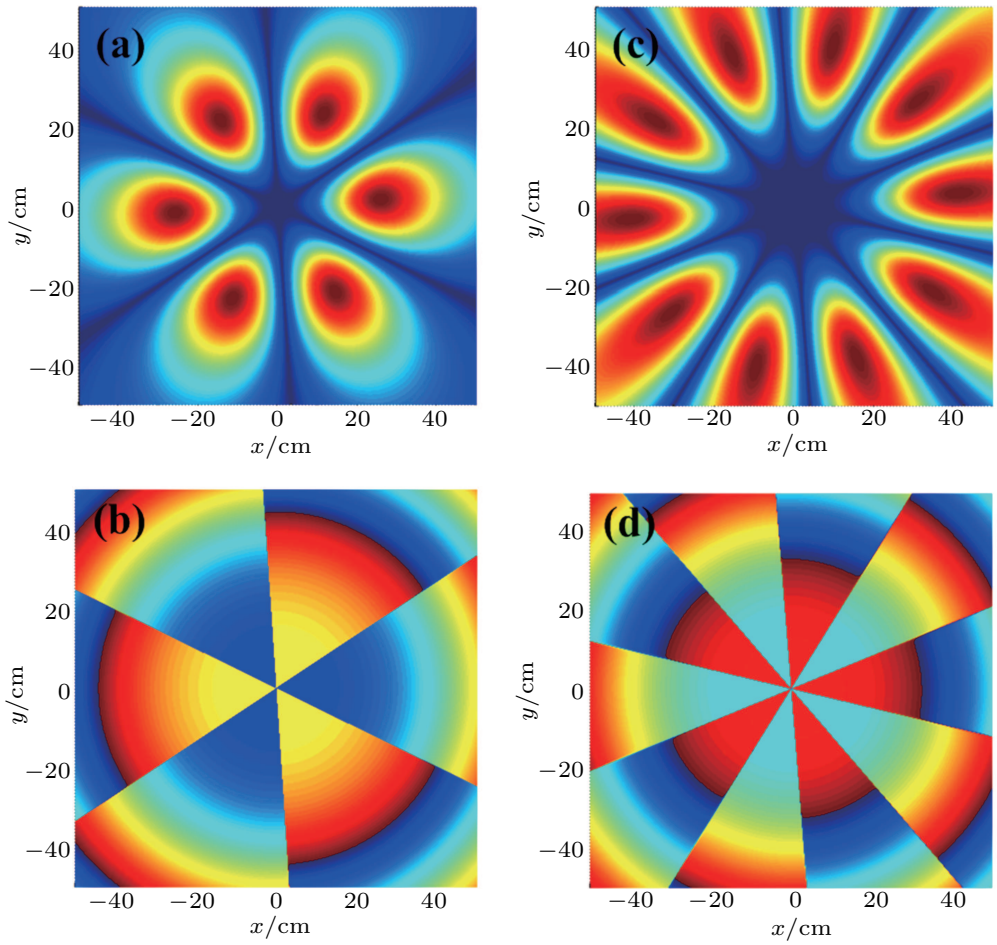


Fig. 7. (color online) Cross-sectional distributions of pressure and phase with obvious edge phase dislocations generated by the coaxial AV beams with ((a) and (b)) $l_{\mathrm{E}} = 3$ and $l_{\mathrm{O}} = -3$, and ((c) and (d)) $l_{\mathrm{E}} = 5$, and $l_{\mathrm{O}} = -5$ for $\Delta\varphi = \pi/16$.

4. Conclusions

In this paper, in order to break through the limit of only one on-axis AV beam with a single topological charge along the center axis, a superimposition algorithm for the generation of multiple off-axis AVs is proposed by using dual coaxial AV beams. By applying the phase-coded approach to the circular array of sparse point sources, two coaxial AV beams are generated simultaneously through using the even- and odd-numbered sources, and a composite acoustic field with an on-axis center-AV and multiple off-axis sub-AVs can be generated for $|l_{\mathrm{E}}| \neq |l_{\mathrm{O}}|$. The generation of edge phase dislocation is theoretically derived and numerically analyzed for $l_{\mathrm{E}} = -l_{\mathrm{O}}$. The numbers and the topological charges as well as the positions of the center-AV and sub-AVs are demonstrated to be determined by the topological charges of the coaxial AV beams. A center-AV with the topological charge of $\min(|l_{\mathrm{E}}|, |l_{\mathrm{O}}|)$ and the topological polarity of $\mathrm{sign}(1/l_{\mathrm{E}} + 1/l_{\mathrm{O}})$ is formed along the center axis. The $|l_{\mathrm{E}} - l_{\mathrm{O}}|$ off-axis sub-AVs with the topological charge of 1 and the topological polarity of $\mathrm{sign}(l_{\mathrm{E}} + l_{\mathrm{O}})$ can also be produced around the center-AV. The favorable results provide the feasibility of generating multiple off-axis AVs, and suggest the potential applications in multi-region particle trapping[40] and object manipulation in biomedical engineering.

References

[1] Nye J F and Berry M V 1974 *Proc. R. Soc. Lond. A* **336** 165
[2] Thomas J L and Marchiano R 2003 *Phys. Rev. Lett.* **91** 244302
[3] Bliokh K Y and Freilikher V D 2006 *Phys. Rev. B* **74** 174302
[4] Lekner J 2007 *Phys. Rev. E* **75** 036610
[5] Marchiano R, Coulouvrat F, Ganjehi L, *et al.* 2008 *Phys. Rev. E* **77** 016605
[6] Santillan AO and Volke-Sepulveda K 2009 *Am. J. Phys.* **77** 209
[7] Soskin M S, Gorshkov VN, Vasnetsov M V, *et al.* 1997 *Phys. Rev. A* **56** 4064
[8] He H, Friese M E, Heckenberg N R, *et al.* 1995 *Phys. Rev. Lett.* **75** 826
[9] Hefner B T and Marston P L 1999 *J. Acoust. Soc. Am.* **106** 3313
[10] Marston P L 2009 *J. Acoust. Soc. Am.* **125** 3539
[11] Zhang P, Li T C, Zhu J, *et al.* 2014 *Nat. Commun.* **5** 4316
[12] Baresch D, Marchiano R, Thomas J L 2013 *J. Acoust. Soc. Am.* **133** 3238
[13] Mitri FG 2013 *Appl. Phys. Lett.* **103** 114102
[14] Zhou Q, Sariola V, Latifi K, *et al.* 2016 *Nat. Commun.* **7** 12764
[15] Friese M E, Enger J, Rubinszteindunlop H, *et al.* 1996 *Phys. Rev. A* **54** 1593
[16] Baresch D, Thomas J L, Marchiano R 2013 *J. Appl. Phys.* **113** 184901
[17] Lin S and Crozier K B 2013 *ACS Nano* **7** 1725
[18] Schmiegelow C T, Schulz J, Kaufmann H, *et al.* 2016 *Nat. Commun.* **7** 12998
[19] Kotlyar VV, Kovalev A A and Porfirev A P 2016 *J. Appl. Phys.* **120** 023101
[20] Guo C S, Zhang Y, Han Y J, *et al.* 2006 *Opt. Commun.* **259** 449
[21] Maleev I D and Swartzlander G A 2003 *J. Opt. Soc. Am. B* **20** 1169
[22] Gan X T, Zhao J L, Liu S, *et al.* 2009 *Chin. Opt. Lett.* **7** 1142
[23] Baumann S M, Kalb DM, Macmillan L H, *et al.* 2009 *Opt. Express* **17** 9818
[24] Huang S J, Gu T T, Miao Z, *et al.* 2014 *Acta Phys. Sin.* **63** 244103 (in Chinese)
[25] Mritri F G 2014 *Phys. Rev. E* **89** 023205
[26] Broadbent E G and Moored W 1979 *Philosoph. Trans. Roy. Soc. B Biol. Sci.* **290** 353
[27] Wu J R 1991 *J. Acoust. Soc. Am.* **89** 2140
[28] Feng X, Gao F and Zheng Y 2013 *Appl. Phys. Lett.* **103** 218101
[29] Wang T, Ke M, Qiu C, *et al.* 2016 *J. Appl. Phys.* **119** 214502
[30] Torr G R 1984 *Am. J. Phys.* **52** 402
[31] Mritri F G 2011 *IEEE Trans. Ultrason. Ferroelectr. Freq. Control* **58** 662
[32] Marzo A, Seah S A, Drinkwater B W, *et al.* 2015 *Nat. Commun.* **6** 8661
[33] Jiang X, Li Y, Liang B, *et al.* 2016 *Phys. Rev. Lett.* **117** 034301
[34] Yang L, Ma Q Y, Tu J, *et al.* 2013 *J. Appl. Phys.* **113** 154904
[35] Zheng HX, Gao L, Ma QY, *et al.* 2014 *J. Appl. Phys.* **115** 084909
[36] Gao L, Zheng H X, Ma Q Y, *et al.* 2014 *J. Appl. Phys.* **116** 024905
[37] Li Y Z, Guo G P, Ma Q Y, *et al.* 2017 *J. Appl. Phys.* **121** 164901
[38] Petrov D V 2001 *Opt. Commun.* **200** 387
[39] Kivshar Y S and Nepomnyashchy A 2000 *Opt. Lett.* **25** 123
[40] Hong Z Y, Geng D L, Qin X P, *et al.* 2017 *Acta Phys. Sin.* **66** 124301 (in Chinese)